Published in final edited form as:
Neurogastroenterol Motil. 2010 August ; 22(8): 901–e235. doi:10.1111/j.1365-2982.2010.01505.x.

Molecular Mechanisms of Cross-inhibition Between Nicotinic Acetylcholine Receptors and P2X Receptors in Myenteric Neurons and HEK-293 cells

Dima A. Decker and **James J. Galligan**
Departments of Biochemistry & Molecular Biology (D.A.D.), Pharmacology & Toxicology and the Neuroscience Program (J.J.G.), Michigan State University, East Lansing, MI, USA

Abstract

Background—$P2X_2$ and nicotinic acetylcholine receptors (nAChRs) mediate fast synaptic excitation in the enteric nervous system. P2X receptors and nAChRs are functionally linked. This study examined the mechanisms responsible for interactions between P2X2 and α3β4subunit-containing nAChRs.

Methods—The function of P2X2 and α3β4 nAChRs expressed by HEK-293 cells and guinea pig ileum myenteric neurons in culture was studied using whole-cell patch clamp techniques.

Results—In HEK-293 cells expressing α3β4 nAChRs and P2X2 receptors, co-application of ATP and ACh caused inward currents that were 56 ± 7% of the current that should occur if these channels functioned independently ($P < 0.05$, $n = 9$); we call this interaction cross-inhibition. Cross-inhibition did not occur in HEK-293 cells expressing α3β4 nAChRs and a C-terminal tail truncated P2X2 receptor (P2X2TR)($P > 0.05$, $n = 8$). Intracellular application of the C-terminal tail of the P2X2 receptor blocked nAChR-P2X receptor cross-inhibition in HEK-293 cells and myenteric neurons. In the absence of ATP, P2X2 receptors constitutively inhibited nAChR currents in HEK-293 cells expressing both receptors. Constitutive inhibition did not occur in HEK-293 cells expressing α3β4 nAChRs transfected with P2X2TR. Currents caused by low (≤30 μM), but not high (≥100 μM) concentrations of ATP in cells expressing P2X2 receptors were inhibited by co-expression with α3β4 nAChRs.

Conclusions—The C-terminal tail of P2X2 receptors mediates cross-inhibition between α3β4 nAChR-P2X2 receptors. The closed state of P2X2 receptors and nAChRs can also cause cross inhibition. These interactions may modulate transmission at enteric synapses that use ATP and acetylcholine as co-transmitters.

Keywords

enteric nervous system; *ion channels*; *synaptic transmission*; *patch clamp*; *acetylcholine*; *ATP*

Nicotinic acetylcholine receptors (nAChRs) and P2X receptors are ligand-gated cation channels that mediate cholinergic and purinergic fast synaptic excitation of enteric neurons (1,2). nAChRs are a member of the Cys-loop receptor family which includes $5\text{-}HT_3$ receptors and $GABA_A$ receptors which are also expressed by enteric neurons. Cys-loop receptors are composed of 5 subunits and each subunit has four transmembrane domains and extracellular N and C-terminal tails (3,4). Neuronal nAChRs are composed of two α and three β subunits; there are eight neuronal α (α2–α9) and three neuronal β (β2–β4) nAChR

Corresponding author: Dr. James J. Galligan Department of Pharmacology and Toxicology Michigan State University East Lansing, MI 48824 USA telephone: (517) 353-4776 fax: (517) 353-8915 galliga1@msu.edu.

subunits (3). In the ENS, the predominant nAChR subtype is composed of α3 and β4 subunits and acetylcholine (ACh) acting at nAChRs is the primary fast excitatory neurotransmitter in the ENS (1,5). P2X receptors belong to a different family of ligand-gated cation channels. P2X receptors are composed of three subunits; each subunit has two transmembrane domains and intracellular N and C-terminal tails. P2X receptors are homomeric or heteromeric receptors composed of one or combinations seven ($P2X_1$–$P2X_7$) subunits (6–9). Enteric neurons express P2X2, P2X3, P2X5 and P2X7 subunits (10–13). ATP acting at P2X receptors contributes to fast synaptic excitation in subsets of enteric neurons and ATP and ACh are co-transmitters at many synapses in the ENS (14–16).

Because P2X receptors and nAChRs are structurally different, they have been assumed to function independently. However, nAChRs and P2X receptors co-expressed by myenteric neurons are linked by a mutually inhibitory mechanism where simultaneous receptor activation causes an excitatory response that is smaller in amplitude than the response that should occur if the receptors functioned independently (of one channel inhibits responses mediated by the other channel, resulting in fewer channels opening than expected, also referred to as cross-inhibition (17,18). This functional interaction occurs between nAChRs and P2X receptors composed of P2X2, P2X3 and P2X4 subunits expressed in HEK-293 cells (19). Functional interactions between nAChRs and P2X receptors are not limited to myenteric neurons as similar interactions occur in guinea pig ileum submucosal neurons (20) and guinea pig (21) and rat sympathetic neurons (22) and in rat PC-12 cells (23). The interaction is also not limited to nAChRs as P2X receptors interact functionally with other Cys-loop family members including 5-HT_3 receptors (24,25) and $GABA_A$ receptors (26,27).

This study examined molecular mechanisms responsible for P2X2 and α3β4 nAChR interaction because these receptors expressed by myenteric neurons and because ACh and ATP mediate fast synaptic excitation at synapses in anally-directed pathways in the myenteric plexus (14,28). We used HEK-293 cells because they do not endogenously express P2X2 and α3β4 nAChRs so they provide a mammalian cell system to investigate specific domains of the receptors which may be responsible for receptor cross-inhibition.

Materials and Methods

Human embryonic kidney (HEK-293) cells

Cells were obtained from American Type Culture Collection and grown in Dulbecco's modified Eagle's medium (DMEM) F-12 containing 10% fetal bovine serum, 10% GluMax (Invitrogen, Carlsbad, CA), and 100 units ml^{-1} penicillin and streptomycin, except for the rat $\alpha_3\beta_4$ nAChR stable HEK-293 cell line which also contained 0.5 mg/ml geneticin (GIBCO, G418). Cells were maintained at 37 °C in a 5% CO_2 atmosphere in a humidified incubator. Cells were passaged once every 3 days when they reached 90% confluence. Transient transfection of cells was accomplished using electroporation. A 0.4 cm Gene Pulser Cuvette (BIO-RAD) was used with 2 μg of total plasmid protein along with 0.2 μg of GFP to help identify transfected cells. We used a Gene Pulser Xcell™ electroporation system (BIORAD). This resulted in 80% transfection efficiency. Afterwards, cells were plated on 35 mm coverslips and maintained in the incubator for 24 hrs before use in electrophysiology experiments. A rat α3β4 nAChR stable HEK-293 cell line was provided by Dr. Yingxian Xiao from Georgetown University (29). A plasmid containing the coding sequence for the rat P2X2 receptor subunit was provided by Dr. Alan North (University of Manchester, Manchester, UK). A plasmid containing the coding sequence for a C-terminal tail truncated rat P2X2 receptor (P2X2TR) were a generous gift from Dr. Boué-Grabot (CNRS Université Victor Segalen Bordeaux, France). Plasmids containing the coding sequences for the murine α3 and murine β4 nAChR subunits were provided by Dr. Jerry A. Stitzel (University of Colorado, Denver Colorado).

Myenteric neurons

Neurons were cultured as described previously (17,22). Two newborn guinea-pigs (<36 hrs old) were killed by severing the major neck blood vessel following halothane anesthesia. The small intestine was removed from the animals and placed in cold (4 °C) Krebs solution of the following composition (millimolar): 117 NaCl; 4.7 KCl; 2.5 $CaCl_2$; 1.2 $MgCl_2$; 1.2 NaH_2PO_4; 25 $NaHCO_3$ and 11 glucose. The longitudinal muscle myenteric plexus was stripped free using a cotton swab and cut into 5 mm pieces. Tissues were digested with 1600 U of trypsin, followed by trituration with a fire-polished Pasteur pipette. After incubation with 2000 U crab hepatopancreas collagenase, the tissues were triturated again. The neurons were resuspended in Eagle's minimum essential medium (MEM) containing 10% fetal bovine serum, gentamicin (10 μg ml^{-1}), penicillin (100 units ml^{-1}) and streptomycin (100 units ml^{-1}) and plated onto sterile, poly-L-lysine coated 35 mm plastic dishes and maintained in an incubator at 37 °C in a 5% CO_2 atmosphere for up to 3 weeks.

Whole cell patch clamp recording

Whole-cell voltage-clamp measurements were obtained at room temperature using standard methods. Coverslips containing cells were placed on a stage of an inverted microscope (Nikon Diaphot, Mager Scientific, Inc. Dexter, MI) using phase-contrast optics. For identifying co-transfected cells, a mercury bulb with excitation wavelength of 495 nm was used with a filter for 520 nm emission. The pipette solution contained (millimolar): 122.5 K-aspartate; 20 KCl; 1 $MgCl_2$; 10 EGTA; 5 HEPES; and 2 ATP. The pH was adjusted to 7.3 with KOH. The extracellular solution was a HEPES-based buffer composed of (millimolar): 155 NaCl; 5 KCl; 2 $CaCl_2$; 1 $MgCl_2$; 10 HEPES; and 12 glucose, pH was adjusted to 7.4 with NaOH. All recordings were made using an Axopatch 200B amplifier (Molecular Devices, Inc. Sunnyvale, CA). Data was acquired using pCLAMP 9.1 software (Molecular Devices). Whole-cell recordings were carried out using patch pipettes with tip resistances of 3–5 MΩ; seal resistances were greater than 1 GΩ. There was a two minute interval between all successive agonist applications at each holding potential, −70 mV for HEK-293 cells and −60 mV for myenteric neurons.

Protein construct expression and purification

pGEX vectors with a GST gene Fusion System were generously provided by Dr. Boué-Grabot from the CNRS Université Victor Segalen Bordeaux, France. We were provided with A pGEX with GST (pGEX-GST) as a control vector along with another vector that contains the C-terminal domain of the P2X2 receptor (P2X2-CT, corresponding to amino acids 365–469). The vectors were heat-shock transformed into $BL21D3^+$ cells and grown on Cam (34ug/ml) and Amp (100ug/ml) LB plates. Transformed clones were first grown in a 10 ml culture (LB media containing Cam and Amp) at 30 °C to an A_{600} of 0.5 and then this was expanded into a 500 ml culture containing Cam/Amp and 20% Glucose. These bacterial cells where grown until A_{600} of 0.6 at which point 0.1 mM isopropylβ-ᴅ-thiogalactoside (IPTG) was added. Cultures were induced for 3 hours at 30 °C and cells were finally collected by centrifugation, snap frozen and stored at −80 °C.

Cell-free extracts (soluble protein fractions of cells disrupted by sonication) from induced cultures were affinity purified on immobilized Glutathione agarose beads (Pierce), 10 fractions were collected. Fractions were checked by SDS-Phage that was silver stained. The two fractions that contained the most protein were pooled and dialyzed overnight at 4°C into the intracellular solution buffer. Bradford assay was performed to determine protein concentration and proteins were also visualized with SDS-Page silver-staining and Western blotting analysis (see Supplemental Material).

Drug application

Drugs were applied onto individual neurons/cells by gravity flow from a linear array of quartz tubes placed near the cell. The distance from the mouth of the tubes to the cells was ~200 μm with the position controlled manually using a micromanipulator. Computer-controlled solenoid valves (General Valve, Fairfield, NJ) were used to gate solution flow through the tubes. Agonist-induced currents were measured as the peak current amplitude. The difference between the predicted sum of the individual peak currents was compared with the current amplitude caused by co-application of two agonists. When constructing ATP and ACh concentration response curves, there was a 4 minute interval between each successive 2 s long agonist application.

Statistics

Data are expressed as the mean ± s.e.m. and "*n*" refers to the number of cells from which the data were obtained. The predicted current amplitude that would occur during agonist co-application was calculated by measuring the peak currents caused by previous individual agonist applications and then summing these values. These data were used for statistical comparisons of actual and predicted currents. Traces illustrating predicted currents were constructed using a simple math function in Origin 8 (OriginLab Corp., Northhampton, MA). Student's *t* test was used to establish significant differences between control and treatment groups. The significance level was $P < 0.05$. EC_{50} is the half-maximal effective concentration and n_H is the slope. Y_{min} and Y_{max} are the minimum and maximum respectively. Agonist concentration-response curves were fit to the following logistic function using Origin:

$$y = \frac{(Y_{min} - Y_{max})}{1 + (x/EC_{50})^{nH}} + Y_{max}$$

RESULTS

Cross-inhibition between P2X2 receptors and α3β4 nAChRs in HEK-293 cells

We used HEK-293 cells stably expressing rat α3β4 receptors and transiently transfected with rat P2X2 receptors to study cross-inhibition. ACh (3 mM) and ATP (1 mM) were first applied individually and peak inward currents were measured. When the agonists were applied simultaneously, the resulting inward current was only 56 ± 7 % (Fig. 1A and 1B, $P < 0.05$, $n = 9$) of the predicted current that would have occurred had the P2X2 receptors and α3β4 nAChRs functioned independently. Subsequent individual re-application of ACh and ATP caused currents that were not statistically different from those elicited before agonist co-application (ACh = 0.9 ± 0.2 nA; ATP = 0.4 ± 0.1 nA; $P > 0.05$).

The $P2X_2$ C-terminal tail mediates cross-inhibition

In the next experiments, we used HEK-293 cells that stably expressed α3β4 nAChRs and that were transiently transfected with a C-terminal tail truncated P2X2 receptor (P2X2TR). This receptor has a stop codon at amino acid 374, truncating a majority of the P2X2 receptor cytoplasmic C-terminal domain. The truncated subunit can assemble into a functional receptor (25). In these cells, currents caused by simultaneous application of ACh and ATP caused an inward current that was not statistically different from the predicted current value (82 ± 6%, $P > 0.05$, $n = 8$, Fig. 1C).

The data described above suggest that the C-terminal domain of the P2X2 receptor is a critical determinant of cross-inhibition. To further test this hypothesis, we used the C-

terminal tail peptide as a competitive antagonist to block cross-inhibition. The peptide is a soluble form of the C-terminal tail of the P2X2 receptor (GST-P2X2-CT for amino acids 365–469). A control peptide containing just the GST construct was also tested. These constructs were expressed and purified via affinity chromatography on glutathione beads. Proteins were eluted, pooled, and verified with silver staining and blotted with anti- P2X2 antibody (with affinity for the P2X2 C-terminal tail amino acids 457–472) and anti-GST (see Supplemental Information). Using a rat $\alpha_3\beta_4$ nAChR HEK-293 stable cell line transiently transfected with rat P2X2 receptors, 50 μg of the GST- P2X2-CT peptide or the control GST protein were added to the whole cell patch pipette recording electrode solution. After the GST-control peptide diffused into the cell, the currents caused individual applications ACh and ATP were 0.72 ± 0.15 and 0.74 ± 0.25 nA, respectively. Subsequent agonist co-application still resulted in cross-inhibition of receptors in which actual current was significantly less than the predicted current (Fig. 2A, n = 6, $P < 0.05$). We next tested the GST-P2X2-CT peptide via intracellular dialysis into cells and individual applications of ACh (1.1 + 0.19 nA) and ATP (0.62 ± 0.19 nA) were followed by agonist co-application. In these studies, the actual current caused by agonist co-application was not different from predicted current obtained by summing the previous individual currents (Fig. 2B, $P > 0.05$, n = 6).

The $P2X_2$ C-terminal tail mediates cross-inhibition in myenteric neurons

Whole cell recordings were obtained from myenteric neurons using pipette solutions that contained the GST-control peptide. The GST-control peptide was allowed to diffuse into cells for 8 minutes. ACh (3 mM) and ATP (1 mM) applied individually caused inward currents of 0.16 ± 0.02 nA and 0.25 ± 0.03 nA respectively. Agonist co-application caused an inward current that was significantly smaller than the predicted current (Fig. 3A, $P < 0.05$, n = 6). Recordings were obtained from a second set of neurons dialyzed with the GST-P2X2-CT peptide for 8 minutes. ACh (3 mM) and ATP (1 mM) were then applied individually and these agonists caused inward currents of 0.17 ± 0.05 nA and 0.07 ± 0.006 nA respectively. Agonist co-application then caused an inward current that was not different from the predicted value (Fig. 3B; $P > 0.05$, n = 6).

Constitutive cross-inhibition

We found that ACh currents in HEK-293 cells stably expressing $\alpha_3\beta_4$ nAChRs alone (2.7 ± 0.2 nA, n = 10) were significantly larger than ACh currents recorded from HEK-293 cells stably expressing $\alpha_3\beta_4$ nAChRs and transiently transfected with P2X2 receptors (1.7 ± 0.2 nA; $P < 0.05$, n = 10, Fig. 4A). This constitutive inhibition did not occur in cells stably expressing α3β4 nAChRs and transiently transfected with C-terminal P2X2TR subunit (Fig 4B, $P > 0.05$, n =16). This indicates that co-transfection with P2X2 receptors does not reduce expression of α3β4nAChRs but instead there is a C-terminal tail mediated interaction of the P2X2 receptor with nAChRs. In HEK-293 cells stably expressing full length $P2X_2$ receptors, ATP (1 mM) currents were 1.9 ± 0.3 nA; when these cells were transiently transfected with α3β4 nAChRs, ATP currents (2.0 ± 0.3 nA, Fig 4C, $P > 0.05$, n =12) were not different from those measured in cells expressing only P2X2 receptors.

It is possible that ATP released from surrounding cells might activate P2X2 receptors causing cross-inhibition of nAChRs. Therefore, recordings were obtained in the presence of the P2 receptor antagonist, pyridoxal-phosphate-6-azophenyl-2',4'-disulfonate (PPADS 10 μM) to block P2X2 receptors. At this concentration, PPADS blocked inward currents caused by exogenously applied ATP (Fig. 4D). In HEK-293 cells only expressing α3β4 nAChRs, PPADS did not alter ACh-induced currents ($P > 0.05$, n= 8, Fig. 5). However, when these cells were transfected with P2X2 receptors, the maximum ACh current was reduced (Fig. 5,

$P < 0.05$, n=21). This effect was not altered by PPADS to block P2X2 receptor activation ($P < 0.05$ compared to initial ACh application, n = 10, Fig. 5).

Co-transfection of full length P2X2 receptors into the α3β4 nAChR cell line also caused a rightward shift in the ACh concentration response curve in these cells. Currents were normalized to the maximum response in each cell and EC_{50} values and Hill coefficients were determined using nonlinear curve fitting (Fig. 6A). The ACh concentration response curve in HEK-293 cells stably expressing $\alpha_3\beta_4$ nAChRs and transiently expressing P2X2 receptors was shifted to the right compared to the concentration response curve obtained in cells stably expressing α3β4 nAChRs only (Fig. 6A, Table 1). The Hill slopes for the ACh concentration response curves were not different in the two types of cell (Table 1). Similar results were obtained when ATP concentration response curves were studied in cells stably expressing P2X2 receptors and transiently expressing α3β4 nAChRs where the ATP concentration response curve was right-shifted in cells expressing both receptors. However, as shown above, the response caused by 1 mM ATP acting at P2X2 receptors was not changed in the presence of α3β4nAChRs. The curve was right shifted due to an increase the steepness of the concentration response curve as indicated by the increased Hill coefficient (Fig. 6B, Table 1).

DISCUSSION

Acetylcholine and ATP are co-transmitters acting at nAChRs and P2X2 receptors on myenteric neurons in anally-projecting nerve pathways. The neurons co-expressing nAChRs and P2X2 receptors in the guinea pig ileum myenteric plexus are likely to be inhibitory motorneurons (10,14,28). While cholinergic-purinergic co-transmission at some enteric synapses is well established in the literature, the functional significance of this synaptic mechanism is not clear. This issue is further complicated by the proposal that nAChRs and P2X receptors are linked in a mutually inhibitory manner in myenteric neurons (17,18). The present study attempted to identify the molecular mechanisms by which P2X2 receptors and α3β4 nAChRs are functionally linked as these receptors are co-expressed at myenteric synapses. Cross-inhibition between P2X2 and α3β4 nAChRs known to occur in myenteric neurons can be reproduced using receptors expressed in HEK-293 cells (19). In the present study we used a mutant P2X2 receptor to identify the molecular components responsible for functional interactions between P2X2 receptors and α3β4 nAChRs.

The $P2X_2$ C-terminal tail is required for cross-inhibition

P2X receptor subunits have two membrane spanning domains with intracellular N- and C-terminal sequences. The length of the C-terminal tail varies among the different P2X subunits (8). We used a mutant P2X2 receptor with the C-terminal tail truncated from 119 down to 21 amino acids in length (P2X2TR)(25) to determine if this portion of the subunit is crucial for cross-inhibition with α3β4 nAChRs. These studies showed that responses caused by simultaneous application of ACh and ATP to cells co-expressing the P2X2TR and α3β4 nAChRs were fully additive suggesting that the C-terminal tail of the P2X2 receptor is required for cross-inhibition. Although similar results were obtained in *Xenopus* oocytes (25) injected with mRNA for α3β4 nAChRs and the P2X2TR, this is the first time that these studies have been done in mammalian cells.

To better understand the role of the P2X2 C-terminal tail, a GST- P2X2-CT construct (corresponding to amino acids 365–469) was expressed in bacteria and purified. After purity was verified, this peptide was utilized to compete for the binding sites between P2X2 and nAChRs. Intracellular dialysis of HEK-293 cells co-expressing P2X2 receptors and α3β4 nAChRs with the GST-P2X2-CT peptide blocked cross-inhibition when the receptors were activated simultaneously. Loss of the functional interaction was not an artifact of peptide

dialysis as the GST-control peptide did not block cross-inhibition. These data demonstrate the central role of C-terminal sequence of P2X2 subunits in the functional interaction with nAChRs in HEK-293 cells. The GST- P2X2-CT construct has been used to block interactions between P2X2 receptors and α3β4 nAChRs, 5-HT_3 and $GABA_A$ receptors in *Xenopus* oocytes (25,30). We have shown for the first time that this peptide blocks interactions between α3β4 nAChRs and P2X2 receptors in myenteric neurons which normally co-express these receptors. These data indicate that the mechanism responsible for receptor interaction is not a function of overexpression of receptors in a heterologous system. The P2X2 C-terminal tail interaction with α3β4 nAChRs that occurs in *Xenopus* oocytes and HEK-293 cells also occurs in myenteric neurons. This result supports the utility of using heterologous receptor expression to study the molecular physiology of receptors expressed by myenteric neurons. In addition, loss of cross-inhibition due to P2X2 receptor truncation or competitive binding with GST-P2X2-CT minimizes the possibility that cross-inhibition is due to signaling mechanisms activated by P2Y or muscarinic receptors that are expressed by both HEK-293 cells and myenteric neurons (30–32). Fluorescence resonance energy transfer analysis of α4β2 nAChRs (brain specific receptors) and P2X2, receptors expressed in HEK-293 cells revealed that the receptors were localized within 100 nm of each other in the plasma membrane (33). These data also support the concept that P2X receptors and nAChRs can form a heteromeric complex.

Cross-inhibition does not require receptor activation

The data discuss above suggest that there is a physical association between α3β4 nAChRs and P2X2 receptors that mediates cross-inhibition when the receptors are activated simultaneously. A new finding presented here is that cross-inhibition does not require receptor activation as cross-inhibition occurs when receptors are co-expressed but not co-activated. These data revealed that the average amplitude of currents caused by a maximum concentration of ACh was smaller in cells co-expressing $\alpha_3\beta_4$ nAChRs and P2X2 receptors versus cells only expressing α3β4 nAChRs. However, constitutive inhibition of nAChR function did not occur when the P2X2TR was co-expressed with α3β4 nAChRs. These data indicate that even in the closed state P2X2 receptors, via the C-terminal tail, inhibit nAChR function. To exclude the possibility that ATP released from surrounding HEK-293 cells activates the $P2X_2$ receptor, we added the P2 receptor antagonist, PPADS, to the extracellular buffer. Even in the presence of maximum PPADS concentrations, constitutive inhibition of nAChR function by co-expressed P2X2 receptors persisted.

To further study constitutive inhibition, ACh concentration response curves were obtained in cells expressing α3β4 nAChRs alone or expressing both α3β4 nAChRs and P2X2 receptors. Co-expression of P2X2 receptors caused a parallel rightward shift (no change in Hill slope) in the ACh concentration response curve. These data suggest that P2X2 receptors reduce the affinity of α3β4 nAChRs for ACh. Somewhat different results were obtained when constitutive inhibition of P2X2 receptor function by α3β4 nAChRs was studied. Co-expression with α3β4 nAChRs inhibited P2X2 receptor function to low but not high concentrations of ATP as reflected in an increase in the Hill slope. This suggests that nAChRs may produce an allosteric effect on P2X2 receptor function perhaps by reducing channel open probability at low ATP concentrations. Although constitutive inhibition has not been reported previously, similar asymmetry in cross-inhibition occurs in *Xenopus* oocytes, where nAChR inhibition by simultaneously activated P2X2 receptors was stronger than inhibition of P2X2 receptor function by simultaneously activated nAChRs (18). A similar asymmetric of inhibition between P2X and $GABA_A$ receptors occurs in dorsal root ganglion neurons when these receptors are activated simultaneously (34). This asymmetry may be based on differences in receptor subunit stoichiometry. P2X receptors are trimeric receptors while nAChRs are pentameric receptors (3,8). The P2X2 receptor C-terminal tail

may interact with the intracellular loop between the third and fourth transmembrane domain of cys-loop receptors (25). Therefore, it is possible that a complex formed between nAChRs and P2X2 receptors could be composed of two P2X2 and only one nAChR. This asymmetry in stoichiometric composition of receptor complexes could account for the asymmetry in cross-inhibition.

Conclusions

The data presented here suggest that P2X2 receptors and nAChRs, which mediate fast synaptic transmission in the ENS interact functionally via formation of a heteromeric complex. The physical interaction alters function of the receptor partner when both receptors are activated by their physiological ligand (ACh and ATP) and also when only one of the two activating ligands is present. This novel finding has implications for co-transmission in the ENS as there could be receptor cross-talk even when only one of the synaptic transmitters is available. This cross-inhibition may regulate neuronal excitability and limit calcium influx during bursts of synaptic activity.

Supplementary Material

Refer to Web version on PubMed Central for supplementary material.

Acknowledgments

We are grateful to Dr. Boue-Grabot (CNRS Université Victor Segalen Bordeaux, France) for providing the P2X2TR plasmid along with the GST-control peptide and GST-P2X2-CT constructs. Dr. Xiao (Georgetown University, Washington D.C.) for donating the α3β4 nAChR stable HEK-293 cell line, and Dr. Alan North (University of Manchester, Manchester, UK) for the $P2X_2$ plasmids. And most importantly, we are very grateful for the Wang lab for its guidance and aid in expressing and purifying the GST peptide constructs.

DAD performed all of the experiments, analyzed the data, prepared the figures and wrote the first draft of the manuscript. JJG participated in design of experiments, analysis of data and editing and preparation of the final version of this paper.

Grants This work was supported by the National Institutes of Health grant #DK57039.

REFERENCES

1. Gallligan JJ, LePard KJ, Schneider DA, Zhou X. Multiple mechanisms of fast excitatory synaptic transmission in the enteric nervous system. J Auton Nerv Syst. 2000; 81:97–103. [PubMed: 10869707]
2. Galligan JJ. Pharmacology of synaptic transmission in the enteric nervous system. Current opinion in pharmacology. 2002; 2:623–629. [PubMed: 12482723]
3. McGehee DS, Role LW. Physiological diversity of nicotinic acetylcholine receptors expressed by vertebrate neurons. Ann Rev Physiol. 1995; 57:521–546. [PubMed: 7778876]
4. Miyazawa A, Fujiyoshi Y, Unwin N. Structure and gating mechanism of the acetylcholine receptor pore. Nature. 2003; 423:949–955. [PubMed: 12827192]
5. Zhou X, Ren J, Brown E, Schneider D, Caraballo-Lopez Y, Galligan JJ. Pharmacological properties of nicotinic acetylcholine receptors expressed by guinea pig small intestinal myenteric neurons. J Pharmacol Exp Ther. 2002; 302:889–897. [PubMed: 12183644]
6. Khakh BS. Molecular physiology of P2X receptors and ATP signaling at synapses. Nature Reviews. 2001; 2:165–174.
7. North RA, Surprenant A. Pharmacology of cloned P2X receptors. Ann Rev Pharmacol Toxicol. 2000; 40:563–80. [PubMed: 10836147]
8. North RA. Molecular physiology of P2X receptors. Physiol Rev. 2002; 82:1013–1067. [PubMed: 12270951]

9. Robertson SJ, Ennion SJ, Evans RJ, Edwards FA. Synaptic P2X receptors. Curr Opin Neurobiol. 2001; 11:378–386. [PubMed: 11399438]
10. Castelucci P, Robbins HL, Poole DP, Furness JB. The distribution of purine $P2X_2$ receptors in the guinea-pig enteric nervous system. Histochem Cell Biol. 2002; 117:415–422. [PubMed: 12029488]
11. Poole DP, Castelucci P, Robbins HL, Chiocchetti R, Furness JB. The distribution of $P2X_3$ purine receptor subunits in the guinea pig enteric nervous system. Auton Neurosci. 2002; 101:39–47. [PubMed: 12462358]
12. Ruan HZ, Burnstock G. The distribution of P2X5 purinergic receptors in the enteric nervous system of mouse. Cell Tissue Res. 2005; 319:191–200. [PubMed: 15551155]
13. Hu HZ, Gao N, Lin Z, Gao C, Liu S, Ren J, Xia Y, Wood JD. P2X7 receptors in the enteric nervous system of guinea-pig small intestine. J Comp Neurol. 2001; 440:299–310. [PubMed: 11745625]
14. Lepard KJ, Galligan JJ. Analysis of fast synaptic pathways in myenteric plexus of guinea pig ileum. Am J Physiol. 1999; 276:G529–G538. [PubMed: 9950828]
15. Nurgali K, Furness JB, Stebbing MJ. Analysis of purinergic and cholinergic fast synaptic transmission to identified myenteric neurons. Neuroscience. 2003; 116:335–347. [PubMed: 12559090]
16. Ren J, Bertrand PP. Purinergic receptors and synaptic transmission in enteric neurons. Purinergic Signal. 2008; 4:255–266. [PubMed: 18368519]
17. Zhou X, Galligan JJ. Non-additive interaction between nicotinic cholinergic and P2X purine receptors in guinea-pig enteric neurons in culture. J Physiol. 1998; 513:685–697. [PubMed: 9824710]
18. Khakh BS, Zhou X, Sydes J, Galligan JJ, Lester HA. State-dependent cross-inhibition between transmitter-gated cation channels. Nature. 2000; 406:405–10. [PubMed: 10935636]
19. Decker DA, Galligan JJ. Cross-inhibition between nicotinic acetylcholine receptors and P2X receptors in myenteric neurons and HEK-293 cells. Am J Physiol. 2009; 296:G1267–1276.
20. Barajas-López C, Espinosa-Luna R, Zhu Y. Functional interactions between nicotinic and P2X channels in short-term cultures of guinea-pig submucosal neurons. J Physiol. 1998; 513:671–83. [PubMed: 9824709]
21. Searl TJ, Redman RS, Silinsky EM. Mutual occlusion of P2X ATP receptors and nicotinic receptors on sympathetic neurons of the guinea-pig. J Physiol. 1998; 510:783–791. [PubMed: 9660893]
22. Nakazawa K. ATP-activated current and its interaction with acetylcholine-activated current in rat sympathetic neurons. J Neurosci. 1994; 14:740–750. [PubMed: 7507984]
23. Nakazawa K, Fujimori K, Takanaka A, Inoue K. Comparison of adenosine triphosphate- and nicotine-activated inward currents in rat phaeochromocytoma cells. J Physiol. 1991; 434:647–60. [PubMed: 2023135]
24. Barajas-López C, Montaño LM, Espinosa-Luna R. Inhibitory interactions between $5\text{-}HT_3$ and P2X channels in submucosal neurons. Am J Physiol. 2002; 283:G1238–48.
25. Boué-Grabot E, Barajas-López C, Chakfe Y, Blais D, Bélanger D, Emerit MB, Séguéla P. Intracellular cross talk and physical interaction between two classes of neurotransmitter-gated channels. J Neurosci. 2003; 23:1246–1253. [PubMed: 12598613]
26. Boué-Grabot E, Toulmé E, Emerit MB, Garret M. Subunit-specific coupling between gamma-aminobutyric acid type A and $P2X_2$ receptor channels. J Biol Chem. 2004; 279:52517–52525. [PubMed: 15456793]
27. Karanjia R, García-Hernández LM, Miranda-Morales M, Somani N, Espinosa-Luna R, Montaño LM, Barajas-López C. Cross-inhibitory interactions between $GABA_A$ and P2X channels in myenteric neurones. Eur J Neurosci. 2006; 23:3259–68. [PubMed: 16820016]
28. Johnson PJ, Shum OR, Thornton PD, Bornstein JC. Evidence that inhibitory motor neurons of the guinea-pig small intestine exhibit fast excitatory synaptic potentials mediated via P2X receptors. Neurosci Lett. 1999; 266:169–72. [PubMed: 10465700]

29. Xiao Y, Meyer EL, Thompson JM, Surin A, Wroblewski J, Kellar KJ. Rat α_3/β_4 subtype of neuronal nicotinic acetylcholine receptor stably expressed in a transfected cell line: pharmacology of ligand binding and function. Mol Pharmacol. 1998; 54:322–333. [PubMed: 9687574]

30. Mundell SJ, Benovic JL. Selective regulation of endogenous G protein-coupled receptors by arrestins in HEK293 cells. J Biol Chem. 2000; 275:12900–12908. [PubMed: 10777589]

31. Gwynne RM, Bornstein JC. Synaptic transmission at functionally identified synapses in the enteric nervous system: roles for both ionotropic and metabotropic receptors. Current Neuropharmacology. 2005; 5:1–17. [PubMed: 18615154]

32. Morno RL, Bornstein JC, Bertrand PP. Synaptic transmission from the submucosal plexus to the myenteric plexus in Guinea-pig ileum. Neurogastroenterol Motil. 2008; 20:1165–1173. [PubMed: 18643893]

33. Khakh BS, Fisher JA, Nashmi R, Bowser DN, Lester HA. An Angstrom scale interaction between plasma membrane ATP-gated P2X2 and alpha4beta2 nicotinic channels measured with fluorescence resonance energy transfer and total internal reflection fluorescence microscopy. J Neurosci. 2005; 25:6911–6920. [PubMed: 16033901]

34. Sokolova E, Nistri A, Giniatullin R. Negative cross talk between anionic $GABA_A$ and cationic P2X ionotropic receptors of rat dorsal root ganglion neurons. J Neurosci. 2001; 21:4958–4968. [PubMed: 11438571]

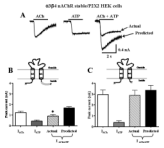

Figure 1.

Truncation of the $P2X_2$ C-terminal tail eliminates cross-inhibition between $P2X_2$ receptors and nAChRs. *A*. Representative traces ATP- (1 mM) and ACh- (3 mM) induced inward currents recorded from $\alpha_3\beta_4$ nAChRs stable HEK-293 cell line transiently transfected with $P2X_2$ receptors. *B*. Pooled data from experiments shown in "A". In cells expressing only the $\alpha_3\beta_4$ nAChR and $P2X_2$ receptors, co-application of ATP and ACh exhibited cross-inhibition (n=9). *Indicates significantly different from the predicted sum of currents ($P < 0.05$, n=8). Inset shows $P2X_2$ subunit with full length C-terminal tail. *C*. $\alpha_3\beta_4$ nAChRs stable HEK-293 cell line transiently with a truncated form of the $P2X_2$ receptor ($P2X_2$TR, inset), cross-inhibition was abolished.

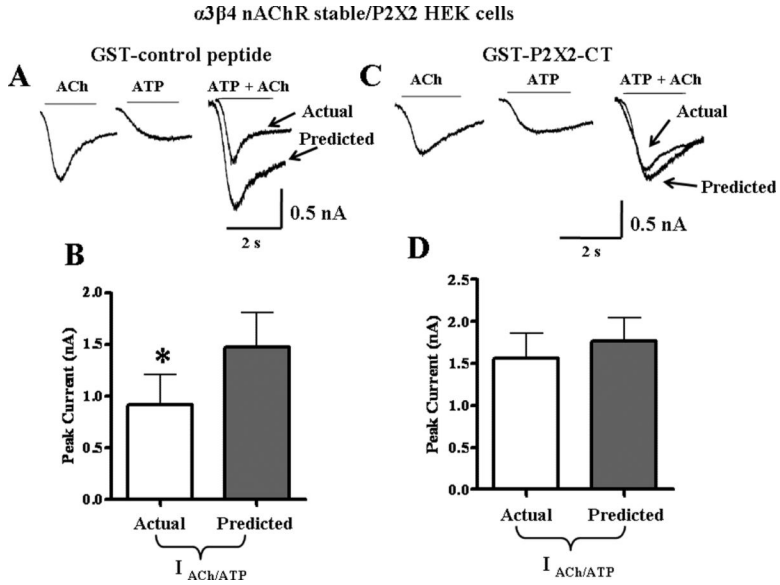

Figure 2.

Cross-inhibition between nAChRs and $P2X_2$ receptors is mediated by the $P2X_2$ receptor C-terminal tail. *A.* Addition of the GST-control peptide to the intracellular electrode did not alter cross-inhibition between nAChRs and $P2X_2$ receptors. *B.* Pooled data (n=6) from experiments shown in A. *Indicates significantly different from the predicted sum of currents ($P < 0.05$). Addition of the GST-$P2X_2$-CT peptide construct (amino acids 365–469) of the $P2X_2$ C-terminal tail to the pipette solution blocks cross-inhibition. *D.* Pooled data from experiments illustrated in "C" (n=6).

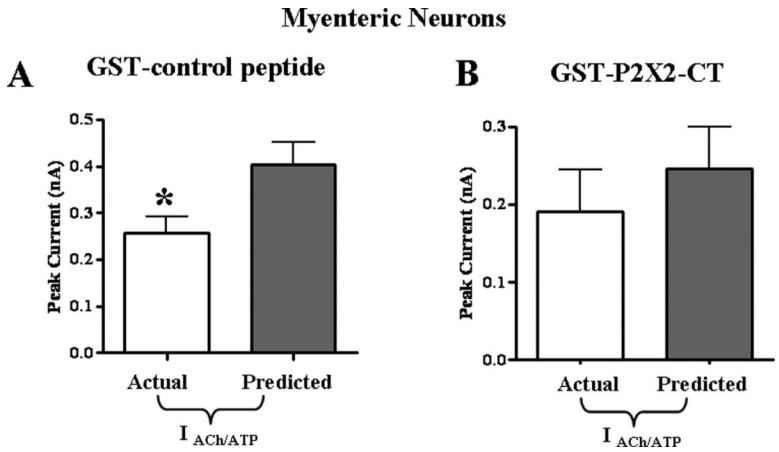

Figure 3.

Cross-inhibition between nAChRs and $P2X_2$ receptors in myenteric neurons is mediated by the $P2X_2$ receptor C-terminal tail. *A.* The GST-control peptide added to the whole cells pipette solution did not block cross-inhibition between nAChRs and $P2X_2$ receptors (n=6). *B.* Addition of the GST-$P2X_2$-CT peptide construct to the pipette solution blocked cross inhibition (n=6). *Indicates significantly different from the predicted sum of currents ($P < 0.05$).

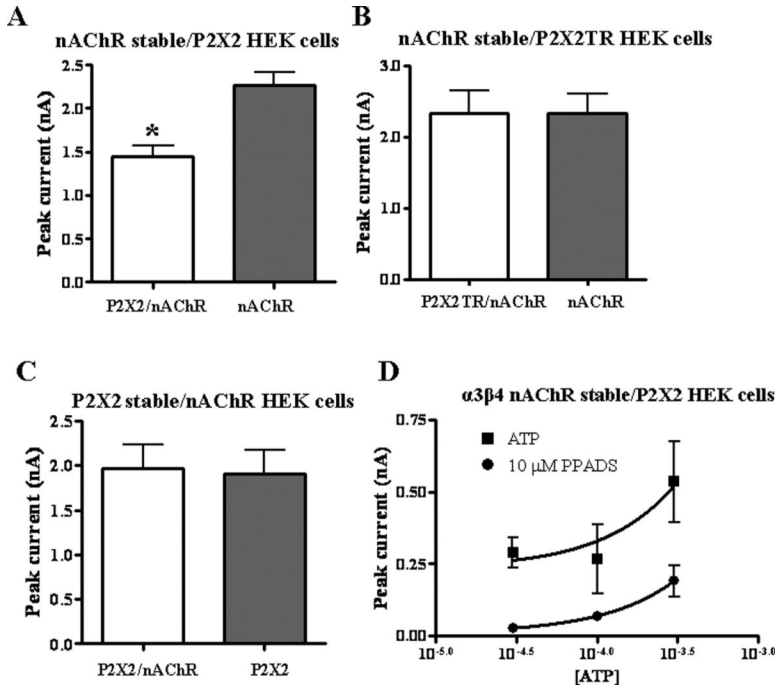

Figure 4.

Constitutive inhibition of nAChRs. *A.* ACh (3 mM) induced currents in cells expressing $\alpha_3\beta_4$ nAChRs alone were larger than when co-expressed with the $P2X_2$ receptor (n=10). *B.* When $\alpha_3\beta_4$ nAChRs were co-expressed with the $P2X_2$ receptor ($P2X_2TR$), ACh induced currents are similar to those recorded from cells expressing only $\alpha_3\beta_4$ nAChRs (n=16). *C.* ATP (1mM) induced currents in cells expressing only $P2X_2$ receptors are similar to those recorded from cells co-expressing P2X2 receptors and $\alpha_3\beta_4$ nAChRs (n=12). *D.* PPADS (10 μM) inhibits ATP induced currents in cells expressing $P2X_2$ receptors. *Indicates significantly different from control currents ($P < 0.05$).

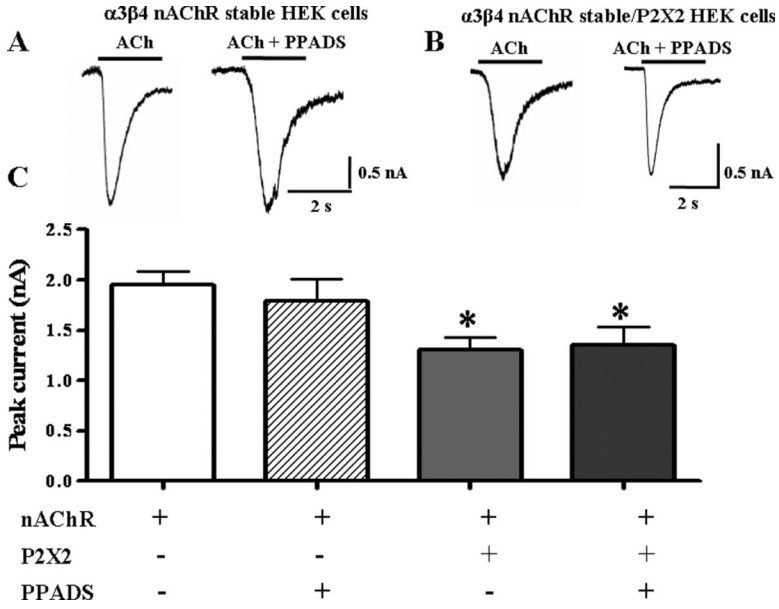

Figure 5. PPADS does not alter $P2X_2$ receptor mediated constitutive inhibition of $\alpha_3\beta_4$ nAChRs

ACh (3mM) induced currents mediated by $\alpha_3\beta_4$ nAChRs expressed individually are not altered by PPADS. However, these currents are inhibited upon co-expression of $\alpha_3\beta_4$ nAChRs with the $P2X_2$ receptor. The addition of PPADS does not alter the constitutive inhibition. `n' indicates the number of cells. *Indicates significantly different from currents of $\alpha_3\beta_4$ nAChRs expressed alone ($P < 0.05$).

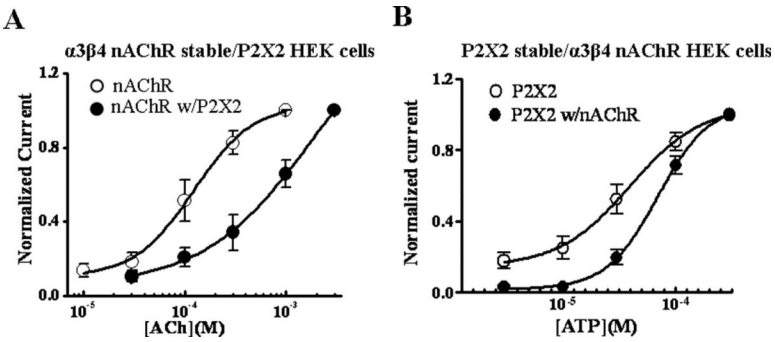

Figure 6. Asymmetric constitutive cross-inhibition between nAChRs and $P2X_2$ receptors

A. Concentration response curves to ACh in cells expressing $\alpha_3\beta_4$ nAChRs alone, and in cells co-expressing $\alpha_3\beta_4$ nAChRs and $P2X_2$ receptors (n=7). P2X2 receptor co-expression caused a parallel rightward shift in the ACh concentration response curve. *B.* ATP concentration response curves in cells expressing $P2X_2$ receptors alone, and in cells co-expressing $\alpha_3\beta_4$ nAChRs and $P2X_2$ receptors (n=5). nAChR co-expression inhibited responses at low but not high ATP concentrations (see Table 1).

Table 1

Half maximal effective concentrations (EC_{50}) and Hill slope values for ACh and ATP concentration response curves in HEK-293 cells expressing nAChRs and P2X2 receptors individually and together.

	EC_{50} (μM)	Hill slope
nAChR stable (n = 9)	172 ± 31	1.6 ± 0.2
nAChR stable with transient P2X2 (n = 6)	471 ± 176*	1.4 ± 0.3
P2X2 stable (n = 4)	34 ± 7	0.8 ± 0.2
P2X2 stable with transient nAChRs (n = 4)	72 ± 7*	1.9 ± 0.3*

Data are mean ± s.e.m. “n” values are the number of cells.

* indicates significantly different from value obtained in cells expressing on one receptor.